SCIENTIFIC REPORTS

OPEN

Drosophila Kruppel homolog 1 represses lipolysis through interaction with dFOXO

Received: 30 June 2017
Accepted: 15 November 2017
Published online: 27 November 2017

Ping Kang[1], Kai Chang[1], Ying Liu[1], Mark Bouska[1], Allison Birnbaum[1], Galina Karashchuk[2], Rachel Thakore[2], Wenjing Zheng[2], Stephanie Post[2], Colin S. Brent[3], Sheng Li[4], Marc Tatar[2] & Hua Bai[1,2]

Transcriptional coordination is a vital process contributing to metabolic homeostasis. As one of the key nodes in the metabolic network, the forkhead transcription factor FOXO has been shown to interact with diverse transcription co-factors and integrate signals from multiple pathways to control metabolism, oxidative stress response, and cell cycle. Recently, insulin/FOXO signaling has been implicated in the regulation of insect development via the interaction with insect hormones, such as ecdysone and juvenile hormone. In this study, we identified an interaction between *Drosophila* FOXO (dFOXO) and the zinc finger transcription factor Kruppel homolog 1 (Kr-h1), one of the key players in juvenile hormone signaling. We found that *Kr-h1* mutants show delayed larval development and altered lipid metabolism, in particular induced lipolysis upon starvation. Notably, Kr-h1 physically and genetically interacts with dFOXO *in vitro* and *in vivo* to regulate the transcriptional activation of insulin receptor (*InR*) and adipose lipase *brummer* (*bmm*). The transcriptional co-regulation by Kr-h1 and dFOXO may represent a broad mechanism by which Kruppel-like factors integrate with insulin signaling to maintain metabolic homeostasis and coordinate organism growth.

Metabolic homeostasis plays important roles in developing animals[1,2]. The ability to coordinate growth and development with nutrient availability is critical for the adaptation to fluctuating environment. The main hormonal pathway that regulates insect growth and energy metabolism is insulin/insulin-like growth factor signaling (IIS). Unlike the single insulin, two insulin-like growth factor (IGF) system in mammals, insects have multiple insulin-like peptides[3,4]. The activation of insulin/insulin-like growth factor signaling stimulates two major kinase cascades: the PI3K/AKT pathway and MAPK/ERK pathways[5]. In particular the O subclass of the forkhead transcription factors (FOXO) are substrates of PI3K/AKT. Decreased cellular IIS leads to de-phosphorylation and nuclear translocation of FOXO and the transcriptional activation of FOXO target genes[6,7]. Besides IIS, FOXO transcriptional activity is modulated by several other pathways (e.g. AMPK, JNK and SIRT) through post-translational modification (PTM) that modulate FOXO binding to DNA or its co-activators[6,7].

FOXO plays a key role in mediating the cross-talk between insulin signaling and other insect hormones (e.g. juvenile hormone (JH) and ecdysteroids) to coordinate insect growth, development and metabolic homeostasis[8–10]. Molting hormone ecdysone regulates developmental timing by inhibiting insulin signaling and promoting the nuclear localization of *Drosophila* forkhead transcription factor (dFOXO)[8]. During the non-feeding pupation stages of *Bombyx* silkworm, 20-hydroxyecdysone (20E) induces lipolysis and promotes transcriptional activation of two adipose lipases via the regulation of FOXO[11]. On the other hand, the link between JH and insulin signaling was first demonstrated in *Drosophila* where insulin receptor (InR) mutants were seen to reduced JH biosynthesis[12]. Recent studies on size control further suggest that JH controls growth rate through *Drosophila* FOXO[10]. Interestingly, JH also regulates lipid metabolism via the interactions with FOXO in Tsetse flies[9] and diapausing mosquitoes[13]. Across these studies, it remains unclear how JH interacts with nutrient signaling and whether JH directly acts on FOXO-mediated transcriptional control.

[1]Department of Genetics, Development, and Cell Biology, Iowa State University, Ames, IA, USA. [2]Department of Ecology and Evolutionary Biology, Brown University, Providence, RI, USA. [3]U.S. Department of Agriculture, U.S. Arid Land Agricultural Research Center, Maricopa, AZ, USA. [4]Key Laboratory of Insect Developmental and Evolutionary Biology, Institute of Plant Physiology and Ecology, Shanghai Institutes for Biological Sciences, Chinese Academy of Sciences, Shanghai, China. Correspondence and requests for materials should be addressed to M.T. (email: Marc_Tatar@brown.edu) or H.B. (email: hbai@iastate.edu)

FOXO interacts with a number of transcription factors within the nucleus to activate or inhibit transcription of target genes[14]. The interactions between FOXO and its binding partners contribute to the transcriptional specificity of FOXO and pleotropic functions of insulin/FOXO signaling. For instance, mouse FOXO1 interacts with PGC-1α in liver to modulate insulin-mediated gluconeogenesis[15]; mammalian FOXO1 binds to Smad2/3 in response to TGF-beta signaling and regulates cell proliferation[16]; mammalian FOXO transcription factors (FOXO3A and FOXO4) interacts with beta-Catenin of Wnt signaling to modulate cellular oxidative response[17]. In *Drosophila*, dFOXO interacts with bZIP transcription factor REPTOR of mechanistic target of rapamycin (mTOR) signaling to regulate growth and energy homeostasis[18]. Interestingly, recent studies found that FOXO interacts with Ultraspiracle (Usp), a co-factor of the ecdysone receptor, to regulate ecdysone biosynthesis and developmental timing in *Drosophila*[19]. To date, factors of JH signaling have not been identified to directly interact with FOXO.

Kruppel-like homolog 1 (Kr-h1) is a key regulator of insect molting and metamorphosis and a major effector in JH signaling[20–22]. JH strongly induces the transcription of *Kr-h1* via its receptor Methoprene-tolerant (Met)[21–23]. During insect development, Kr-h1 functions as a transcriptional repressor on neurogenesis of mushroom body and photoreceptor maturation[24,25]. Kr-h1 belongs to Kruppel-like factors (KLFs) protein family, a group of conserved C2H2 type zinc finger transcription factors. Unlike mammalian KLFs that contain three zinc finger DNA binding domains, *Drosophila* Kr-h1 has eight zinc finger motifs[26]. KLFs are also closely related to transcription factor Sp1 (specificity protein 1). At least seventeen KLFs are identified in mammals[27]. Both KLFs and Sp1-like factors recognized GC-rich DNA elements or CACCC-box in the promoters of target genes[27]. While KLFs and Sp1 can function as both transcription activator and repressor, the N-terminus of KLFs contains a consensus motif PXDL(S/T) that is thought to interact with transcriptional co-repressor CtBP (C-terminal binding protein)[28,29]. Some KLFs also interact with transcriptional co-activators to enhance transcriptional activities. For instance, KLF1 is acetylated through its interaction with co-activators p300 and CREB-binding protein (CBP), which leads to elevated induction of target gene beta-globin[30].

In this study, we identified an interaction between dFOXO and the zinc finger transcription factor Kr-h1 in *Drosophila*. While characterizing a *Kr-h1* mutant, we found that lipolysis was elevated in fasting mutant larvae. Genetic and molecular analyses revealed that Kr-h1 physically interacts with dFOXO and represses the transcriptional activation of dFOXO target genes, such as insulin receptor (*InR*) and adipose triglyceride lipase (*bmm or brummer*). The present study suggests a mechanism by which Kruppel-like factor Kr-h1 integrates with insulin/dFOXO signaling to control lipid metabolism and coordinate organism growth.

Results

***Kr-h1* mutants delay larval development and have reduced triglyceride.** Here we study the role of *Drosophila* Kruppel-like factor Kr-h1 in larval development and metabolic control using a P-element-induced hypomorphic allele *Kr-h1*[*7*] (also known as *Kr-h1*[*k04411*])[20,31]. The P-element insertion is located within the first intron of the *Kr-h1* locus and is reported to interfere with the transcription of *Kr-h1* isoforms. *Kr-h1*[*7*] homozygous mutants are partially viable during embryonic and larval development[31]. We backcrossed this *Kr-h1*[*7*] allele into a yw^R background for seven generations. The heterozygotes of cleaned *Kr-h1*[*7*] mutants showed prolonged developmental time to pupariation (Fig. 1A), while the homozygotes arrest at either second or third instar larval stage. *Kr-h1* mRNA is largely reduced in homozygous animals based on primers for the common region of all three isoforms (Fig. 1B). Using a newly generated anti-Kr-h1 antibody, three major bands were detected in larval samples from wild-type and *Kr-h1*[*7*] heterozygotes (Fig. 1C). Each of these bands was significantly reduced in homozygous animals (Fig. 1C). In the *Drosophila* genome, there are three Kr-h1 isoforms. The predict molecular weight of Kr-h1 is 85.6 kDa for the α and γ isoforms, and 91.5 kDa for the β isoform[20,31]. In Fig. 1C, top band is probably the α isoform (the most abundant isoform at larval stages) because this band corresponds to the recombinant Kr-h1α protein purified using a HaloTag Protein Expression System (Fig. 1D). The nature of two lower bands in Fig. 1C is unclear, probably reflecting cross-reactivity of our Kr-h1 antibodies with other *Drosophila* proteins, or proteolysis events of the Kr-h1 protein. The latter might be more likely because we observed a reduction of the intensity of all three bands in *Kr-h1*[*7*] mutants (Fig. 1C).

Defects in metabolic regulation also occur in the developmentally delayed *Kr-h1* mutants. Using Nile red staining, we found that the fat body lipid droplet was slightly enlarged in *Kr-h1*[*7*] homozygous mutants, despite their smaller nuclear size (Fig. 1D). Upon fasting (16 hours in 1x PBS), the size of lipid droplet was reduced in both wild-type and *Kr-h1* mutants. To quantify fat reserves, we performed a colorimetric assay of triglycerides (TAG), the major form of lipid storage in the fat body, using larvae at 90 hours after egg laying (AEL). Among fed animals, triglycerides were reduced 2-fold by *Kr-h1* mutation, while glycogen was similar among genotypes (Fig. 1F and G). TAG is a major stored nutrient mobilized during fasting. Fasting reduced TAG stores in both genotypes, but to a significantly greater extent in *Kr-h1*[*7*] homozygous larvae (2.9-fold vs 1.4-fold in wild-type) (Two-way ANOVA, interaction $p < 0.047$). Fasting reduced stored glycogen to the same extent in both genotypes (Fig. 1F and G).

In flies, adipose triglyceride lipase brummer (*bmm*) is a key lipase involved in TAG mobilization[11,32]. While transcripts of *bmm* were slightly up-regulated by fasting in wild-type larvae (Fig. 1H), its expression was dramatically increased in fasted *Kr-h1*[*7*] homozygous larvae (4.3-fold vs. 1.8-fold in wild-type) (Two-way ANOVA, interaction $p < 0.0196$) (Fig. 1H). This result is consistent with the greater TAG mobilization in fasted *Kr-h1* mutants as shown in Fig. 1F, suggesting that lipase activities might be enhanced in *Kr-h1* mutants, especially upon fasting. In parallel, transcripts of fly perilipin *Lsd-1* were upregulated in *Kr-h1* mutants and down-regulated in both genotypes upon fasting (Fig. 1I). Perilipin proteins (PLINs) are a group of lipid droplet-associated proteins that act as protective coating factors to prevent lipid breakdown by triglyceride lipases[33,34]. The elevated *Lsd-1* transcripts in *Kr-h1* mutants is consistent with the enlarged lipid droplet observed in Fig. 1E. Notably, repression of *Lsd-1* by fasting was significantly enhanced in *Kr-h1* mutants (10.2-fold vs. 2.4-fold in wild-type) (Two-way

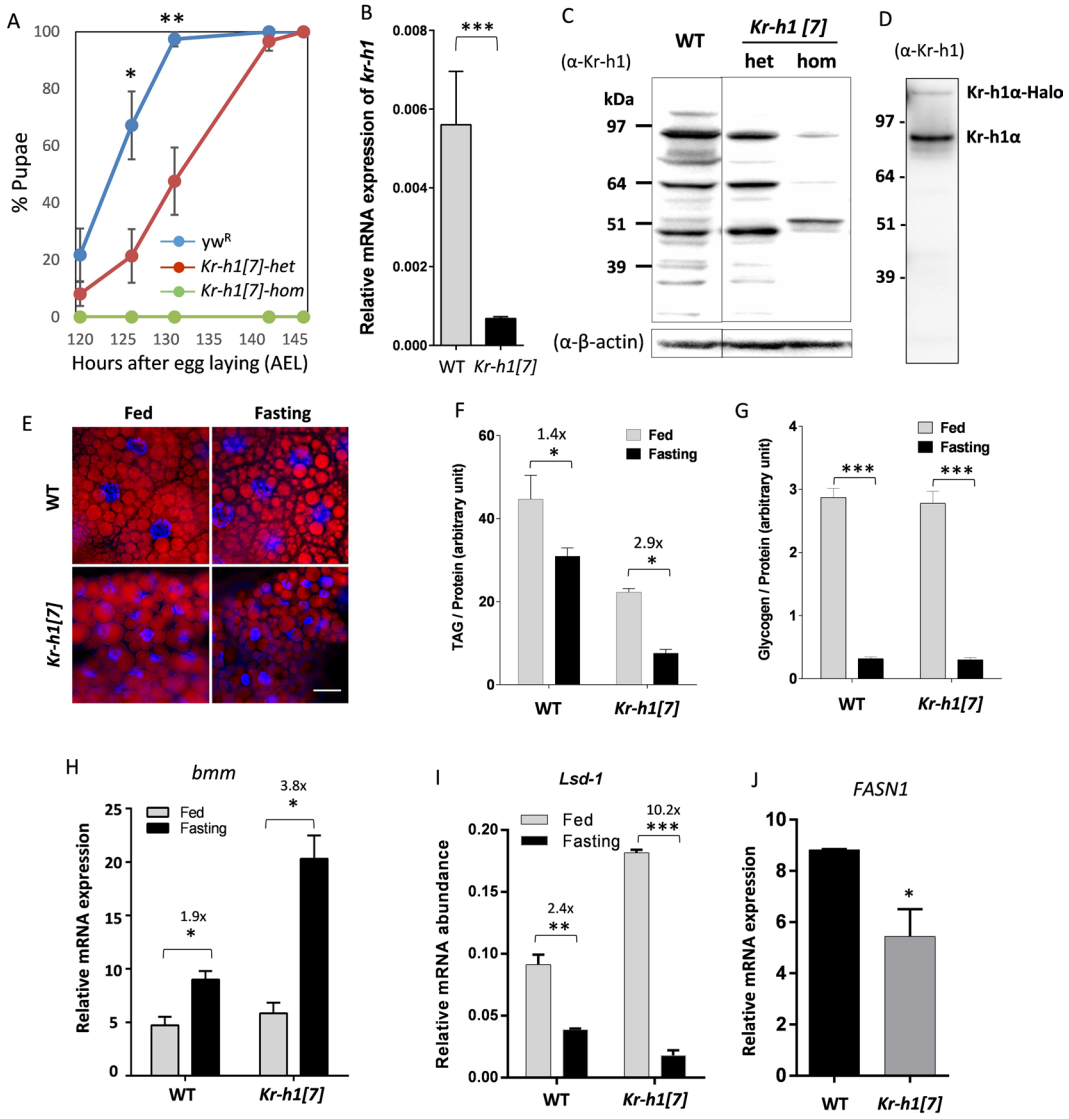

Figure 1. *Kr-h1* mutants delayed larval development and have reduced triglyceride. (**A**) *Kr-h1*[*7*] heterozygous mutants delayed pupation and homozygotes arrested at early larval stages. Percentage of pupariation at different developmental time points is shown. Data are represented as mean ± SE of three trials. Student t-test (**p < 0.01, *p < 0.05). (**B**) *Kr-h1* transcripts were significantly down-regulated in *Kr-h1*[*7*] mutants. Primers targeting common regions among three isoforms were used in qRT-PCR. Each bar represents mean ± SE of three biological replicates. Statistical significance between wild-type and mutants is assessed by student t-test (***p < 0.001). (**C**) Reduced Kr-h1 protein expression in *Kr-h1*[*7*] homozygous mutants. Larvae at 90 hr AEL (after egg laid) were used in western blots. (**D**) Western blot for recombinant Kr-h1α isoform (second band). The top band is uncleaved Kr-h1α-Halo fusion protein. (**E**) Nile red staining of fat body lipid droplet in wild-type and *Kr-h1*[*7*] homozygous mutants. Nuclear staining is in blue. Scale bar: 20 μm. (**F**) *Kr-h1* mutant larvae have reduced TAG level. Upon starvation, TAG mobilization was faster in Kr-h1 mutants than in wild-type larvae. Larvae at 90 hr AEL were fasted for 16 hr in culture vials with wet kimwipe soaked with PBS. Each bar represents mean ± SE of three biological replicates. Statistical significance is assessed by two-way ANOVA followed by Tukey multiple comparisons test (***p < 0.001, **p < 0.01, *p < 0.05). (**G**) Glycogen contents and the utilization rate were not affected by *Kr-h1* mutation. (**H**) Transcripts of TAG lipase *brummer* (*bmm*) were up-regulated by fasting and *Kr-h1* mutation. The fasting-induced *bmm* expression was further enhanced by *Kr-h1* mutation. (**I**) Fasting-triggered fly perilipin *Lsd-1* repression was significantly enhanced in *Kr-h1* mutants. Statistical significance is assessed by two-way ANOVA followed by Tukey multiple comparisons test (***p < 0.001, **p < 0.01, *p < 0.05). (**J**) The expression of *FASN1* (Fatty acid synthase 1) was reduced in *Kr-h1* mutants. Student t-test (*p < 0.05).

ANOVA, interaction $p < 0.0001$). In addition, we observed a reduced expression of *FASN1* (Fatty acid synthase 1) in *Kr-h1* mutants (Fig. 1J). FASN1 is the major enzyme in condensation of acetyl-CoA and malonyl-CoA to palmitic acid and palmitoyl-CoA during fatty acid biosynthesis. Since the expression of TAG lipase *bmm* was

not altered in fed *Kr-h1* mutants (Fig. 1H), it is likely that the reduction of TAG in *Kr-h1* mutants is through the regulation of *FASN1* expression and lipogenesis, rather than lipolysis.

Collectively, these results suggest that Kr-h1 plays an important role in lipid metabolism. Upon fasting, Kr-h1 regulations lipolysis through the transcriptional regulation of triglyceride lipase *bmm*, and lipid droplet-associated protein *Lsd-1*. In contrast, Kr-h1 acts on lipogenesis under normal fed condition. The present study focuses on the role of Kr-h1 in lipolysis under nutrition deprivation.

***Kr-h1* mutants have reduced insulin signaling.** One way Kr-h1 might modulate TAG is through interactions with insulin/IGF signaling. Insulin/IGF signaling is a metabolic master regulator that controls lipase gene expression through its downstream transcription factor dFOXO[35]. Here we see that phosphorylation of IIS-regulated kinase AKT was reduced in *Kr-h1*[*7*] homozygotes (Fig. 2A). Furthermore, *Kr-h1*[*7*] homozygotes had reduced expression of two insulin-like peptides (*dilp2* and *dilp5*), which are the major DILPs produced from brain neurosecretory cells, known as insulin producing cells (IPCs) (Fig. 2B and C).

Reduced insulin signaling is expected to activate forkhead transcription factor dFOXO[6]. Accordingly, mRNA expression of two key dFOXO target genes, *4ebp* (eukaryotic translation initiation factor 4E binding protein) and *InR* were significantly induced in *Kr-h1* mutants (Fig. 2D and E), and *InR* expression was further increased in fasted *Kr-h1*[*7*] homozygotes (5.2-fold vs. 3.4-fold in wild-type) (Two-way ANOVA, interaction $p = 0.1023$) (Fig. 2F). It is known that the transcription of *InR* is controlled by dFOXO through a negative feedback mechanism[36]. Thus, in *Kr-h1* mutant larvae, insulin signaling is inhibited and dFOXO is activated. Kr-h1 may produce these effects in two ways: Kr-h1 regulates the expression of dFOXO target genes via transcriptional co-regulation and direct interaction with dFOXO, or through indirect modulation of insulin/AKT signaling and the expression of *dilp2* and *dilp5*.

***Kr-h1* genetically interacts with *dfoxo* to regulate the transcription of *InR* and *bmm*, and lipid metabolism.** To determine if dFOXO is required for Kr-h1 to mediated lipid metabolism, we generated a double mutant by combining *Kr-h1*[*7*] and *dfoxo*[*21*][37]. Interestingly, we found that *dfoxo*[*21*] heterozygotes rescued the delayed pupariation of *Kr-h1*[*7*] heterozygous mutants (Fig. 2G). As well, *dfoxo*[*21*] mutants suppressed the elevated *InR* and *bmm* expression found in *Kr-h1*[*7*] mutants (Fig. 2H and I), confirming that these transcription factors co-regulate key metabolic genes. Furthermore, the reduction of TAG in *Kr-h1*[*7*] homozygous mutants was rescued by *dfoxo*[*21*]−/− (Fig. 2J). Together, these results reveal a genetic interaction between Kr-h1 and dFOXO in the control of the transcription of metabolic genes and lipid metabolism.

Kr-h1 physically interacts with dFOXO. Kr-h1 and dFOXO may interact directly or indirectly to regulate the expression of *InR* and *bmm*. To test the possibility of direct interaction, we co-immunoprecipitated (Co-IP) Kr-h1 and dFOXO in cultured *Drosophila* cells. We were able to pull down endogenous dFOXO from nuclear and cytoplasmic extracts using an anti-dFOXO antibody. Interestingly, Kr-h1 was detected in the protein complex from the nuclear extracts, but not from the cytoplasmic extracts (Fig. 3A), suggesting that Kr-h1 can form a protein complex with dFOXO in the nuclei.

To identify the protein interaction site between these transcriptional factors, we cloned a series of deletion fragments that contained different protein domains into the Gateway expression vectors. Both the DNA binding domain and transactivation domain of dFOXO bound to full-length Kr-h1 proteins (Fig. 3B). On the other hand, the Kr-h1 fragments that contain transactivation/repression domain (a Q-rich domain) bound to full-length dFOXO proteins, while Kr-h1 fragments with no Q-rich domain showed no binding (Fig. 3C). Therefore, the transactivation/repression domain of Kr-h1 is responsible for the interaction between Kr-h1 and dFOXO.

The direct interaction between dFOXO and Kr-h1 may provide a mechanism for the transcriptional repression of dFOXO target genes by Kr-h1. To test this idea, we co-expressed dFOXO with Kr-h1 (or Kr-h1 Q-rich domain) in Kc167 cells. The mRNA expression of *bmm* was significantly induced by dFOXO alone, and this induction was blocked by co-expressing either full-length of Kr-h1 or Q-rich domain (Fig. 3D). Thus, Kr-h1 appears to repress dFOXO transcriptional activity through direct protein-protein interactions.

Kr-h1 binds to the promoters of *insulin receptor* and *brummer* lipase adjacent to dFOXO binding sites. Kr-h1 and dFOXO physically interact and may thus transcriptionally co-regulate metabolic genes. It has been previously shown that dFOXO binds to the promoter regions near transcriptional start sites of *InR* and *bmm*[35,36], although our recent ChIP-Seq analysis (unpublished) suggests that dFOXO also strongly bound the promoter region near the 5′-UTR of *InR* (P1 region as shown in Fig. 4A) that contains a canonical FOXO binding motif (GTAAATAA). To identify potential Kr-h1 response elements of *InR* and *bmm*, we searched their promoters using mammalian KLF motifs in the Jaspar database (http://jaspar.genereg.net). Three putative KLF binding sites denoted P1~P3 in each promoter were identified including sites in 5′-UTR and intronic regions (Fig. 4A and B) (Supplementary Table S1). We did not find any sites corresponding to the *Bombyx* Kr-h1 response element (GACCTACGCTAACGCTAAATAGAGTTCCGA) reported by Kayukawa *et al.*[23].

Binding of dFOXO and Kr-h1 to these putative sites was determined by ChIP-PCR analysis in fasted animals. At *InR*, dFOXO binding was strongest in the P1 region located at the 5′-UTR region (Fig. 4C), while Kr-h1 bound most strongly to the P3 regions, about 15k bp away from P1 region (Fig. 4D). At *bmm* lipase, both dFOXO and Kr-h1 bound with highest affinity in the P1 region (Fig. 4E and F). The co-localization of Kr-h1 and dFOXO binding suggests these factors could interact at promoters to control the transcriptional activation of the key metabolic genes (e.g., *bmm* lipase).

Kr-h1 represses dFOXO binding to the promoter of *InR* and *bmm*. Kr-h1 may repress dFOXO activity by inhibiting its binding at response elements in *bmm* and *InR*. We performed a ChIP-PCR to test this possibility using anti-dFOXO antibody and *Kr-h1*[*7*] mutants. dFOXO binding to the *InR* P1 region was increased from

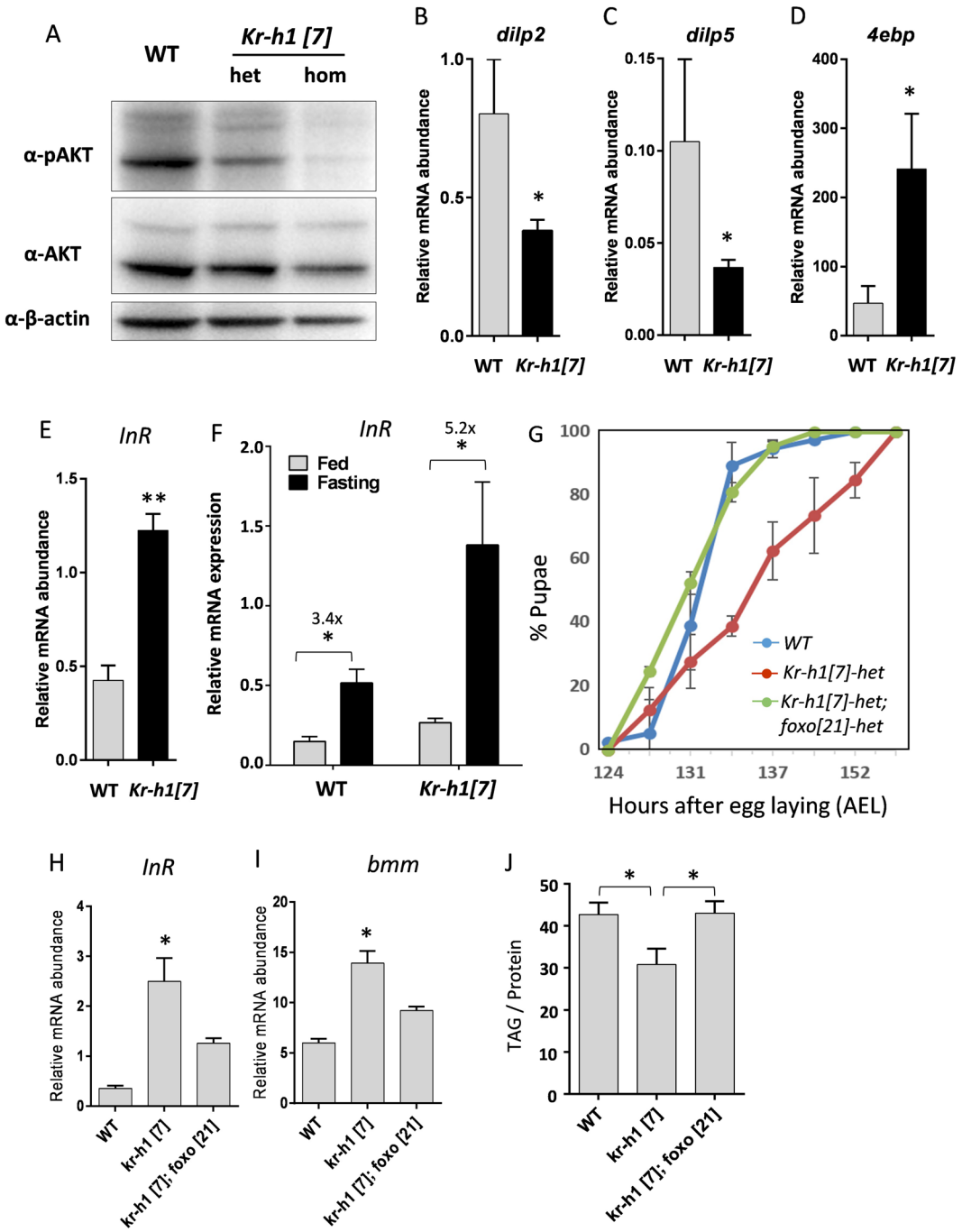

Figure 2. *Kr-h1* mutants have reduced insulin signaling. (**A**) Phosphorylation of AKT was down-regulated in *Kr-h1* mutants. Ten 90 hr AEL larvae were lysed in RIPA buffer and ~20 μg of denatured protein was loaded to SDS-PAGE gels. (**B**,**C**) The transcripts of two insulin-like peptides (*dilp2*, *dilp5*) were down-regulated by *Kr-h1* mutation. (**D**,**E**) The mRNA expression of the key dFOXO targets *4ebp* and *InR* were up-regulated in *Kr-h1* mutants. Each bar represents mean ± SE of three biological replicates. Statistical significance between wild-type and mutants is assessed by student t-test (**$p < 0.01$, *$p < 0.05$). (**F**) *InR* transcripts is additively regulated by fasting and Kr-h1. Statistical significance is assessed by two-way ANOVA with Tukey multiple comparisons test (***$p < 0.001$, **$p < 0.01$, *$p < 0.05$). (**G**) The delayed pupariation of *Kr-h1*[*7*] heterozygous mutants is rescued by *foxo*[*21*] mutants. (**H**) *dfoxo*[*21*] mutants suppress the induction of *InR* transcription by *Kr-h1*[*7*]. (**I**) *dfoxo*[*21*] mutants suppress the induction of *bmm* transcription by *Kr-h1*[*7*]. Each bar represents mean ± SE of three biological replicates. (**J**) *dfoxo*[*21*] mutants rescue the reduction of TAG levels in *Kr-h1*[*7*] mutants. Statistical significance is assessed by one-way ANOVA, followed by Dunnett's multiple comparisons (*$p < 0.05$).

2.9-fold relative to negative control (Act5C) in fasted wild-type to 8.95-fold in fasted *Kr-h1* mutants (Two-way ANOVA, interaction $p < 0.0001$) (Fig. 4G). In contrast, dFOXO binding to the *bmm* P1 region was slightly but

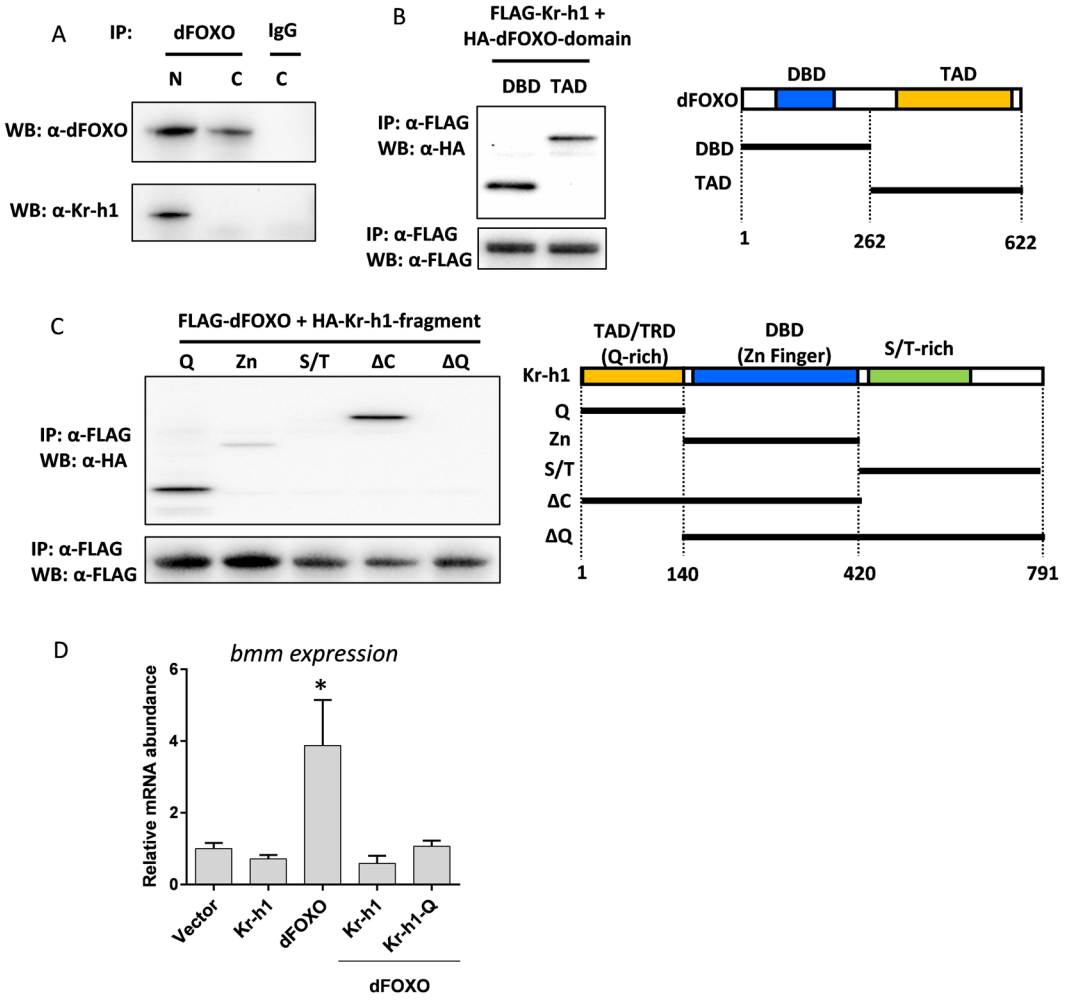

Figure 3. Kr-h1 physically interacts with dFOXO. (**A**) Co-immunoprecipitation of endogenous dFOXO and Kr-h1 from Kc167 cell lysates (N: Nuclear extracts; C: Cytoplasmic extracts). Anti-dFOXO antibodies were used in pull-down. Rabbit IgG served as a negative control. (**B**) Co-immunoprecipitation of FLAG-tagged full-length Kr-h1 and HA-tagged dFOXO fragments. Anti-FLAG antibodies were used to pull-down. Schematic graph on the right showing the position of each dFOXO fragment. Both DNA binding domain and transactivation domain of dFOXO are able to bind to Kr-h1. (**C**) Co- immunoprecipitation of FLAG-tagged full-length dFOXO and HA-tagged Kr-h1 fragments. Anti-FLAG antibodies were used to pull down Kr-h1-dFOXO complex Schematic graph on the right showing the position of each Kr-h1 fragment. Q-rich domain shows strong binding to dFOXO. TAD/TRD: Transactivation/repression domain. DBD: DNA binding domain. (**D**) Expression of either full-length Kr-h1 or Q-rich domain in Kc167 cells blocked dFOXO-induced transcription of *bmm*. Data are represented as mean ± SE of three trials. One-way ANOVA, followed by Dunnett's multiple comparisons (*$p < 0.05$).

non-significantly increased from 2.1-fold in fasted wild-type to 2.8-fold in fasted *Kr-h1* mutants (Two-way ANOVA, interaction $p = 0.5862$) (Fig. 4H). At the *InR* promoter in particular, inhibition of dFOXO-DNA interaction may be one mechanism by which Kr-h1 modulates dFOXO transcriptional activity. Notably, in a reciprocal experiment with anti-Kr-h1 antibody, the binding of Kr-h1 to *InR* and *bmm* promoters was abolished in *dfoxo*[*21*] mutants (Fig. 4I and J). These data suggest that Kr-h1 may be recruited after dFOXO binds to the promoters of target genes, and Kr-h1 subsequently modulates the transcriptional activities of dFOXO through interfering with dFOXO-DNA interactions.

Kr-h1 expresses in adipose tissue to control larval development and lipid metabolism. To determine where Kr-h1 and dFOXO interact *in vivo*, we examined the nuclear co-localization of Kr-h1 and dFOXO in larval fat body using our anti-Kr-h1 antibodies. Previous studies showed that Kr-h1 expressed broadly in many tissues during late larval and prepupal stages, including imaginal discs, trachea, central nervous system, ring gland, salivary gland, muscle, gut, and fat body[38], and the expression was primarily detected in nuclei. We find that in early L3 larval development, Kr-h1 is expressed at low level and primarily in cytosol (Fig. 5A). We also observed cytoplasmic expression of Kr-h1 in Kc167 cells under normal culture condition (Supplementary figure S6). Interestingly, nuclear co-localization of dFOXO and Kr-h1 was increased in fasted larval fat body (90

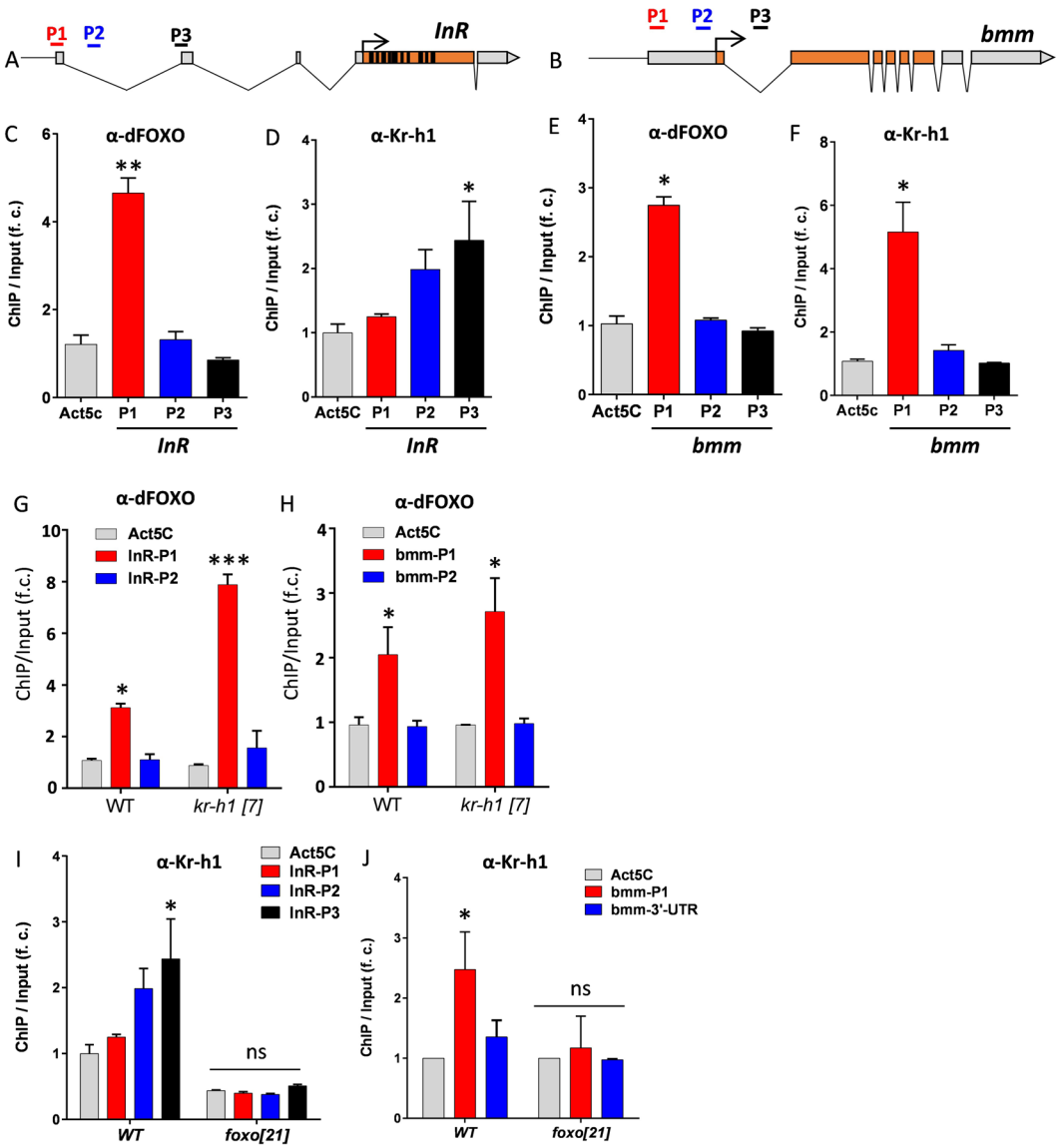

Figure 4. Kr-h1 binds to the promoter of brummer lipase and insulin receptor adjacent to dFOXO binding sites. (**A**) Schematic graph shows insulin receptor (*InR*) locus. P1 region contains a canonical FOXO binding motif (GTAAATAA), while putative mammalian Kruppel binding sits are found in all three regions (based on motif search on the Jaspar database, jaspar.genereg.net). (**B**) Schematic graph shows brummer lipase (*bmm*) locus. P1, P2 and P3 are corresponding to the target sites tested in ChIP-PCR analysis. P1 region contains a canonical FOXO binding motif, while putative mammalian Kruppel binding sits are found in all three regions. (**C**) ChIP-PCR analysis on dFOXO binding to *InR* promoter. (**D**) ChIP-PCR analysis on Kr-h1 binding to *InR* promoter. Each bar represents mean ± SE of three biological replicates. Statistical significance is assessed by one-way ANOVA. (**E**) ChIP-PCR analysis on dFOXO binding to *bmm* promoter. (**F**) ChIP-PCR analysis on Kr-h1 binding to *bmm* promoter. (**G**) dFOXO binding to *InR* promoter (P1 region) is enhanced in fasted *Kr-h1* mutants. Interaction is statistically significant, $p < 0.0001$. (**H**) dFOXO binding to *bmm* promoter (P1 region) is slightly enhanced in fasted *Kr-h1* mutants. Interaction is not statistically significant, $p = 0.5862$. (**I**) Kr-h1 binding to *InR* promoter is abolished in fasted *dfoxo*[*21*] mutants. (**J**) Kr-h1 binding to *bmm* promoter is abolished in fasted *dfoxo*[*21*] mutants. Each bar represents mean ± SE of three biological replicates. Statistical significance is assessed by one-way ANOVA, followed by Dunnett's multiple comparisons (*$p < 0.05$, ns: not significant).

hr AEL) (Fig. 5A). We verified the specificity of our Kr-h1 antibody and found no nuclear expression of Kr-h1 in *Kr-h1*[*7*] homozygous mutants (Fig. 5B). Thus, dFOXO and Kr-h1 may interact in fat body nuclei to co-regulate the transcriptional activation of target genes.

dFOXO expressed in fat body regulates local lipid metabolism and the production of Dilp2 from brain IPCs[39]. To determine where Kr-h1 acts to regulate lipid metabolism and larval development, we knocked down *Kr-h1* message through RNA interference (RNAi) with tissue-specific Gal4 drivers. Knockdown of *Kr-h1* in fat body (r4-gal4) and muscle (Mhc-gal4) delayed pupariation, while knockdown in gut, IPCs and Corpus allatum

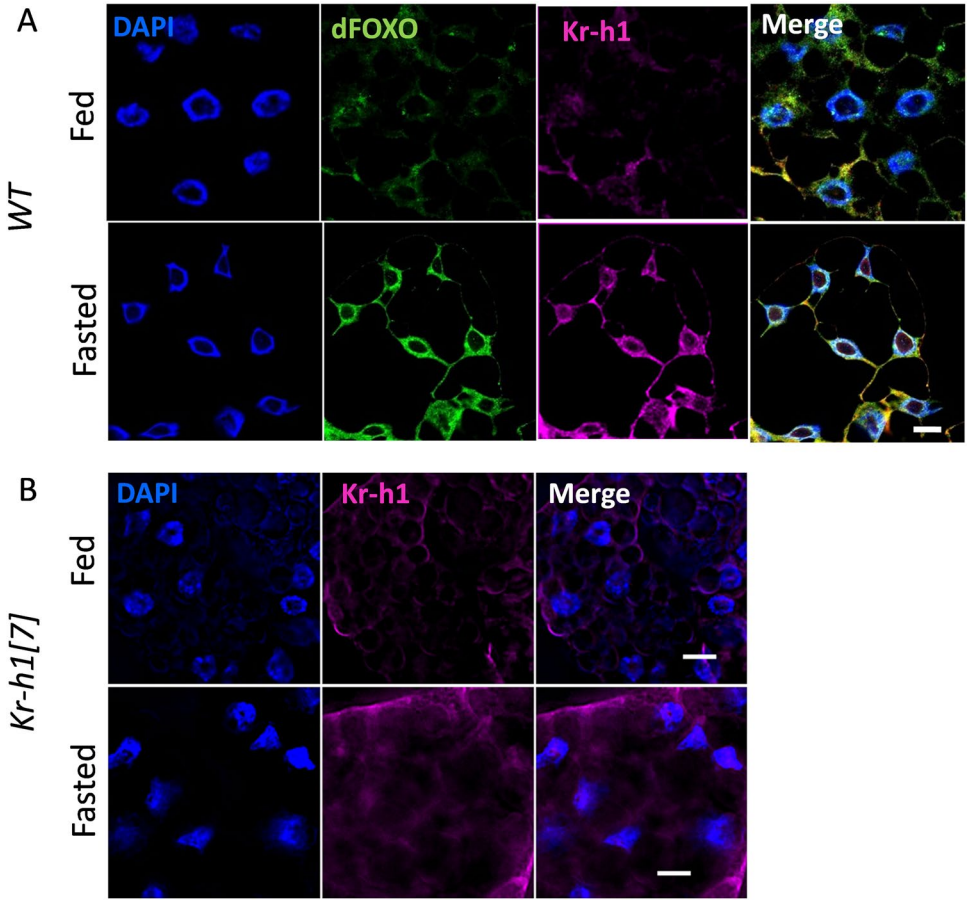

Figure 5. Nuclear co-localization of Kr-h1 and dFOXO in larval fat body. (**A**) Nuclear co-localization of Kr-h1 and dFOXO in fat body upon fasting. Larvae at 90 hr AEL were fasted for 16 hr in culture vials with wet kimwipe soaked with 1x PBS. Fat body cells were dissected and staining with anti-Kr-h1 and anti-dFOXO antibodies. (**B**) Fasting-induced nuclear translocation of Kr-h1 was not observed in *Kr-h1*[*7*] mutants. Scale bar: 10 μm.

(CA) showed no effects on larval development (Fig. 6A). Since fat body is the major site for triglyceride storage in *Drosophila*, we further examined the role of Kr-h1 in the regulation of lipid metabolism in this tissue. Fat body-specific knockdown of *Kr-h1* induced *bmm* transcription, while overexpression of *Kr-h1* repressed it (Fig. 6B). *Kr-h1* expressed in fat body also increased whole larval TAG levels (Fig. 6C). Thus, adipose-expressed *Kr-h1* is essential for larval development and metabolic regulation.

Juvenile hormone signaling regulates lipase *bmm* through dFOXO. The interaction between Kr-h1 and dFOXO has the potential to integrate development and nutrient signaling. Nutrient signaling through FOXO involves insulin, AMPK, SIRT and JNK in both insect and mammals alike[6,14]. On the other hand, the upstream regulators of Kruppel-like factors are poorly characterized in vertebrates, but among insects Kr-h1 is decisively regulated by JH, a key hormonal signal involved in molting and metamorphosis[21]. In particular, JH induces the transcription of *Kr-h1* via the JH receptor Methoprene-tolerant (Met)[22,40]. In this capacity, recent studies suggest that JH and Met are involved in not only development programming, but also in metabolic control[9,41–43], although how JH affects metabolism is largely unknown.

Given that Kr-h1 and dFOXO functionally interact to control lipid metabolism, we examined if this feature provides a way for JH to affect metabolic regulation through *bmm* transcription. Consistent with previous studies[9], triglyceride levels were reduced in flies where the corpora allata were genetically ablated (CAX) (Fig. 7A). Conversely, wild-type flies exposed to the JH analog (JHA) methoprene had elevated TAG contents compared to controls (Fig. 7B). Additionally, *Met* mutations down-regulated TAG levels (Fig. 7C) and up-regulated *bmm* mRNA (Fig. 7D). Met also genetically interacts with dFOXO to regulate the mRNA expression of *bmm* (Fig. 7D). JH may therefore regulate *bmm* through a Met-mediated interaction with dFOXO. Supporting this prediction, methoprene treatment inhibited the expression of *bmm* in wild-type flies, but not in *dfoxo*[*21*] mutants (Fig. 7E). Furthermore, fasting reduced JH titers about 2-fold in both female and male flies (Fig. 7F). But while it is known that JH positively regulates Kr-h1 transcription[21,23], *Kr-h1* mRNA was not reduced upon fasting (Fig. 7G). On the other hand, methoprene treatment was sufficient to induce *Kr-h1* transcription (Fig. 7H). Overall these results indicate that JH signaling interacts with dFOXO to regulate lipid metabolism and lipase gene expression, but the mechanistic role of Kr-h1 in this process remains to be elucidated.

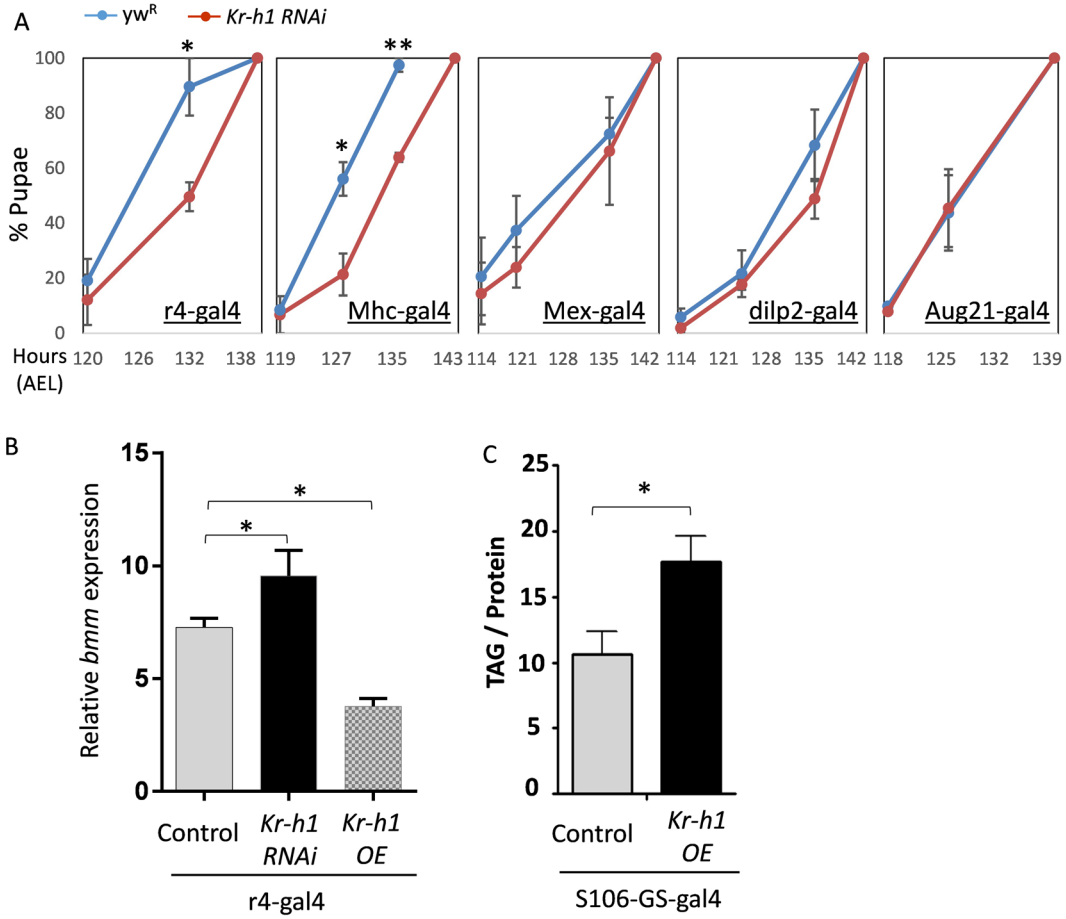

Figure 6. Fat body-expressed *Kr-h1* regulates larval development and lipid metabolism. (**A**) Knockdown of *Kr-h1* expression in fat body (r4-gal4) and muscle (Mhc-gal4) delayed the pupariation. Knockdown of *Kr-h1* in gut (Mex-gal4), IPCs (dilp2-gal4) and CA (Aug21-gal4) shows no effects on larval development. The Kr-h1 RNAi line was backcrossed into a yw^R background for five generations prior to developmental timing experiments. Data are represented as mean ± SE of three trials. Student t-test (**$p < 0.01$, *$p < 0.05$) (**B**) Fat body-specific knockdown of *Kr-h1* induced *bmm* transcription, while overexpression of *Kr-h1* in fat body repressed it. (**C**) Fat body-specific overexpression of *Kr-h1* increased TAG levels. Data are represented as mean ± SE of three trials. Student t-test or one-way ANOVA (*$p < 0.05$).

Discussion

Transcriptional coordination is a key process contributing to metabolic homeostasis[44]. Multiple transcription factors interact at their genomic binding sites to enhance transcriptional specificity and pleiotropic functions of metabolic pathways. As a key node in the metabolic network, forkhead transcription factor FOXO has been shown to interact with diverse transcription co-factors and thereby integrate signals to control metabolism and oxidative stress[6,14]. Intriguingly, in recent genomic studies[45–47], enriched FOXO binding at specific genes does not always correlate to elevated transcriptional output, suggesting there exists inhibitory or inertial mechanisms to repress the transcriptional activity of DNA-bound FOXO.

Here we find that *Drosophila* Kruppel-like factor Kr-h1 acts as a repressor of dFOXO to modulate induction of two dFOXO target genes, *InR* and *bmm*. Like other FOXO interacting partners, Kr-h1 physically binds to dFOXO and inhibits the expression of dFOXO targets by influencing the binding affinity of dFOXO to DNA. The transcriptional activity of FOXO is typically regulated in two layers. The first and probably most important regulation is through PTM, including phosphorylation, acetylation and ubiquitination[6]. PTM of FOXO proteins can affect its subcellular localization (by phosphorylation), DNA binding affinity (by acetylation) and protein degradation (by ubiquitination). Interestingly, the effects of acetylation on FOXO factors seem to be quite different from those by acetylation on KLFs. Acetylation of FOXO by co-factor CBP/p300 weakens the FOXO binding to its DNA targets[48], while CBP/p300 acetylated KLF1 shows increased transcriptional activation of target gene beta-globin[30]. The second mechanism for the regulation of FOXO activity is through the interaction between FOXO and other transcription factors or co-factors. FOXO factors have been shown to interact with diverse transcription factors (e.g. Smad3/4, PGC-1α, STAT3) that often potentiate the expression of FOXO target genes[14]. Kr-h1 identified in our study presents another example for this type of modulatory regulation, although the interaction between Kr-h1 and dFOXO results in transcription repression, instead of activation.

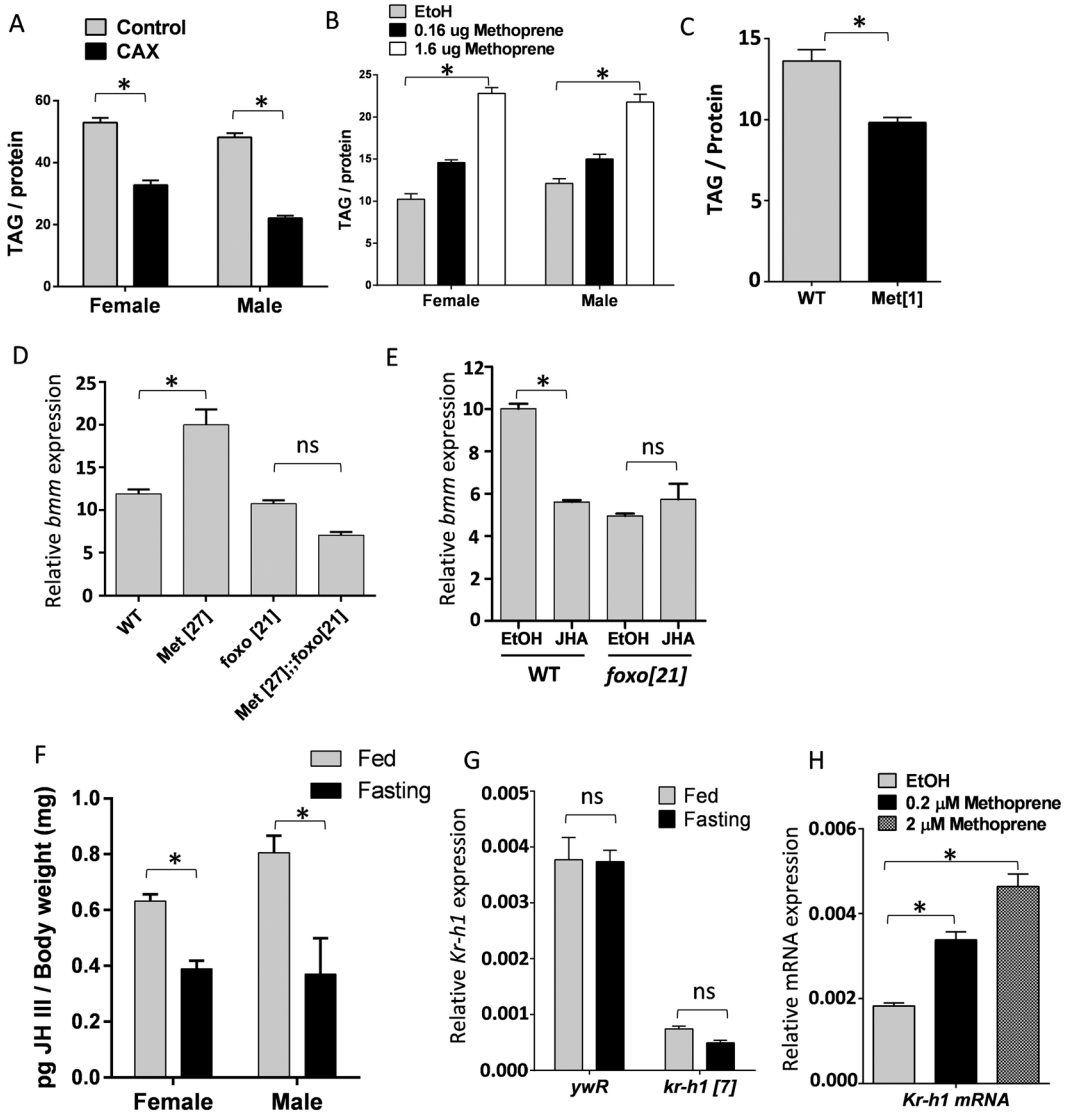

Figure 7. Juvenile hormone signaling regulates TAG lipase *bmm* through dFOXO. (**A**) TAG levels are reduced in CA ablation (CAX) flies. Each bar represents mean ± SE of three biological replicates. Student t-test (*$p < 0.05$). (**B**) Flies exposed to JH analog (JHA) methoprene show increased TAG levels. Each bar represents mean ± SE of three biological replicates. One-way ANOVA (*$p < 0.05$). (**C**) *Met* mutants have reduced TAG levels. Student t-test (*$p < 0.05$). (**D**) Genetic interaction between *Met* and *dfoxo* in the regulation of *bmm* transcripts. *bmm* transcription is up-regulated in *Met* mutants, which was rescued by *dfoxo*[21] mutants. One-way ANOVA (*$p < 0.05$, ns: not significant). (**E**) JH analog (JHA) methoprene treatment led to reduced *bmm* expression in wild-type female flies, but not in *dfoxo*[21] mutant flies. Each bar represents mean ± SE of three biological replicates. Statistical significance is assessed by two-way ANOVA (*$p < 0.05$, ns: not significant) (**F**) JH titer is decreased upon fasting. 10-day-old adult flies were fasted (in culture vial with wet kimwipe soaked with PBS) for 16 hours before collected for JH quantification. Each bar represents mean ± SE of 5~7 biological replicates. Statistical significance is assessed by student t-test (*$p < 0.05$). (**G**) The mRNA expression of *Kr-h1* did not change upon fasting. (**H**) Methoprene treatment induced *Kr-h1* transcription. Each bar represents mean ± SE of three biological replicates. One-way ANOVA (*$p < 0.05$, ns: not significant).

While we do not fully resolve how Kr-h1 blocks dFOXO activity, it seems that Kr-h1 can inhibit dFOXO binding to its DNA targets. This result is similar to previous studies showing reduced FOXO-DNA binding upon interaction with androgen receptor (AR)[49] and with peroxisome proliferator-activated receptor-γ (PPARγ)[50]. Alternatively, Kr-h1 may act by inhibiting recruitment of dFOXO-coactivators (e.g. SIRT or CBP/p300) or by sequestering these coactivators away from dFOXO. Kr-h1 may also recruit additional co-repressors (e.g. CtBP or Sin3-HDAC) to the dFOXO transactivation sites to block the transcriptional activation of target genes. The N-terminal Q-rich domain of KLFs is crucial for the recruitment of co-repressors CtBP and Sin3A[51]. In our co-immunoprecipitation assays, the Q-rich domain of Kr-h1 strongly binds to dFOXO, suggesting Kr-h1 might inhibit dFOXO activity through recruiting co-repressors. One possible candidate is an Sds3-like gene (CG14220), which was previously found to co-immunoprecipitate with Kr-h1[52]. Sds3-like gene family proteins can form

co-repressor complex with Sin3A and HDAC to inhibit gene transcription via interactions with sequence-specific transcription factors[53].

KLFs have well documented roles in cell proliferation, differentiation and apoptosis[51]. The function of Kr-h1 in lipid metabolism and insulin signaling identified in the present study complements recent studies where KLFs function in cellular metabolic regulation, such as gluconeogenesis[54,55]. Likewise, KLF15 deletion in mice produces hypoglycemia and impaired amino acid catabolism upon fasting[55]. Additionally, KLF5 heterozygous mice are resistant to high-fat diet-induced obesity. SUMOylation modulates the transcriptional activities of KLF5 and its association with peroxisome proliferator-activated receptor-delta (PPAR-delta) to control the expression of carnitine-palmitoyl transferase-1b (Cpt1b), uncoupling proteins 2 and 3[56]. Interestingly, KLF4 has recently been identified as a direct target gene of FOXO-mediated transcription during B cell development[57], suggesting a potential interaction between KLF and FOXO transcriptional regulatory network.

Our ChIP-PCR studies suggest that *Drosophila* KLF Kr-h1 transcriptionally controls many metabolic genes, including key dFOXO targets (e.g. *InR* and triglyceride lipase *bmm*). While it is not known whether *Drosophila* Kr-h1 could broadly interact with dFOXO across the genome, such a genome-wide interaction between mammalian FOXO factors and KLFs has been suggested by a recent meta-analysis[58]. Because Kr-h1 plays an important role in morphogenesis during *Drosophila* development[21], the interplay between Kr-h1 and dFOXO raises the possibility that Kr-h1 coordinates growth and development through insulin/dFOXO-mediated metabolic regulation.

We also noticed that the direct interaction between Kr-h1 and dFOXO occurs strongly upon fasting. In the normal fed state, transcriptional regulation of lipase *bmm* is weakly regulated by Kr-h1, although the TAG is significantly reduced in fed *Kr-h1*[*7*] mutants. We speculate that decreased TAG in *Kr-h1*[*7*] mutants is probably due to the reduction in lipogenesis and fatty acid synthesis, rather than to increased lipolysis. Our preliminary data reveal that the expression of fatty acid synthase is down-regulated in *Kr-h1*[*7*] mutants. The potential connection between Kr-h1 and lipogenesis needs to be further examined.

In insects, Kr-h1 is one of the key effectors of JH signaling, an important hormonal pathway governing insect molting, metamorphosis and reproduction. Recent studies reveal that JH also participates in the regulation of carbohydrate and lipid metabolism[9,41–43,59,60]. In Tsetse flies, JH and insulin co-regulate the expression of TAG lipase and inhibit lipolysis[9], which is consistent with our observation that TAG metabolism and lipase *brummer* expression are regulated by JH and its receptor Met. Similarly, JH III treatment reduced FOXO levels in diapause-destined female mosquitoes, *Culex pipiens*[13]. Although we did not test the paralog of Met, germ cell-expressed (GCE)[61–63], previous studies have demonstrated GCE is not involved in lipid metabolism during lactation state of Tsetse flies[9]. Finally, JH signaling was recently found to genetically interact with insulin/dFOXO to control larval growth rate and define final body size in *Drosophila*[10]. Thus, the transcriptional co-regulation of lipid metabolism by *Drosophila* Kr-h1 and dFOXO may contribute to a novel mechanism through which JH interacts with insulin signaling to integrate metabolism and growth during larval development.

Since both Kr-h1 and dFOXO express highly in metabolic tissues (fat body and muscle) of *Drosophila*, these transcription factors are likely to co-regulate many key metabolic genes. As well, these metabolic tissues contribute significantly to other insect physiology and organismal functions, such as stress resistance and aging that are tightly regulated by insulin/dFOXO signaling[64] and by JH signaling[41]. We predict that the interplay between Kr-h1 and dFOXO will also contribute to the regulation of these adult physiological processes. In fact, a recent study reported that loss of kruppel-like factors (KLFs) abolished the lifespan extension in multiple longevity paradigms in *C. elegans*, such as dietary restriction and insulin receptor mutant *daf-2*[65]. Thus, identifying the key co-factors, mechanisms, and downstream events of the Kr-h1/dFOXO transcriptional network may advance our understanding of how JH and insulin signaling coordinately regulate metabolism, development, and aging.

Materials and Methods

Fly Husbandry and Stocks. Flies were maintained at 25 °C, 40% relative humidity and 12-hour light/dark. Adults were reared on agar-based diet with 0.8% cornmeal, 10% sugar, and 2.5% yeast (unless otherwise noted). Fly stocks used in the present study are: *Kr-h1*[*7*] or *Kr-h1* [*k04411*][20,31] (Bloomington # 10381, backcrossed to yw^R), *Kr-h1* RNAi lines (Bloomington # 50685, VDRC #107935), *Kr-h1* EP line #EP2289[24,66], UAS-Kr-h1-LacZ[25], *foxo*[*21*][67], *Met*[*1*][68], *Met*[*27*][68], r4-gal4 (Bloomington # 33832), Mhc-gal4[69], Mex-gal4[70], dilp2-gal4[71], Aug21-gal4[72], S106-GS-gal4[73]. Double mutants were made by crossing *Kr-h1*[*7*] or *Met*[*27*] to *foxo*[*21*] respectively. Corpus allatum (CA) ablation flies (named CAX flies) are generated in our laboratory as previously described[41]. yw^R flies were used as wild-type flies in most of the experiments. For methoprene treatment, adult flies were exposed for 24~48 hours to various concentrations of methoprene applied to the side of culture vials.

Kr-h1 Antibody, Kr-h1 recombinant protein synthesis and Western Blot. Kr-h1 polyclonal antibody was generated in rabbits against the short peptide sequence 'LIEHFKRGDLARHG' (Covance, Dedham, MA, USA) and affinity purified (Thermo Fisher Scientific, Waltham, MA, USA). The specificity of Kr-h1 antibody was verified by western blots (Fig. 1) and immunostaining (Fig. 5) using *Kr-h1* [*7*] mutants. Recombinant Kr-h1α protein was produced and purified using the HaloTag Protein Expression System (Promega, Madison, WI, USA). Kr-h1α cDNA clone (LD32311) was obtained from DGRC (Drosophila Genomics Resource Center) and cloned into pFN29K His_6HaloTag T7 Flexi vector. The Kr-h1α-Halo fusion protein was expressed in Single Step (KRX) Competent Cells and purified using HaloLink Resin (Promega, Madison, WI, USA).

All western blots were performed per the following procedures: Fly tissues or cells were homogenized in RIPA buffer (Thermo Fisher Scientific, Waltham, MA, USA) with protease inhibitors (Sigma-Aldrich, St Louis, MO, USA). Supernatant was incubated with NuPAGE LDS loading buffer (Thermo Fisher Scientific, Waltham, MA, USA) at 70 °C for 10 min. About 20 μg of denatured protein was separated on 4~12% Bis-Tris precast gels (Thermo Fisher Scientific, Waltham, MA, USA) and transferred to PVDF membranes. Following incubation with primary and secondary antibodies, the blots were visualized with Pierce ECL Western Blotting Substrate (Thermo

Fisher Scientific, Waltham, MA, USA). Other antibodies used in the present study are Phospho-*Drosophila* Akt antibody (Ser505) (#4054S, Cell Signaling Technology, Danvers, MA, USA), Akt antibody (#9272S, Cell Signaling Technology).

Quantitative RT–PCR. Total RNA was extracted using Trizol reagent (Thermo Fisher Scientific, Waltham, MA, USA) from 10~15 synchronously staged larvae or whole adult flies. DNase-treated total RNA was quantified and about 500 ng of total RNA was reverse transcribed to cDNA using iScript cDNA Synthesis Kit (Bio-Rad, Hercules, CA, USA). QPCR was performed with an ABI prism 7300 Sequence Detection System (Thermo Fisher Scientific, Waltham, MA, USA). Three to five biological replicates were used for each experimental treatment. mRNA abundance of each gene was normalized to the expression of ribosomal protein L32 (*RpL32* or *rp49*) by the method of comparative C_T. Primer sequences are listed in Supplementary Table S2.

Pupariation timing analysis. Synchronized eggs were placed on 35 × 10 mm petri dishes containing standard medium (see above) at 20~30 eggs per dish. The numbers of pupae were recorded 2~3 times every day around 120 hr AEL till all larvae molt into pupae.

Nile red staining. Larval fat body were dissected in 1x PBS and stained with 0.00005% Nile Red (Sigma-Aldrich, St Louis, MO, USA) and 1 μg/ml Hoechst 33342 (ImmunoChemistry Technologies, Bloomington, MN, USA) in 75% glycerol for 10 min at room temperature. Fat body was then mounted in 75% glycerol and imaged using an Olympus BX51WI upright epifluorescence microscope.

Metabolic assays. All metabolic analyses were performed as previously described[73,74]. For TAG assay, 25 staged larvae or six adult flies were collected and homogenized in 1xPBS containing 0.1% Tween 20 and TAG was quantified using Thermo Scientific™ Triglycerides Reagent (Thermo Fisher Scientific, Waltham, MA, USA). For glycogen measurement, samples were digested with amyloglucosidase (Sigma-Aldrich, St Louis, MO, USA) and glucose contents were quantified using Thermo Scientific™ Glucose Hexokinase Reagents (Thermo Fisher Scientific, Waltham, MA, USA). The relative level of each metabolite was obtained by normalizing the metabolites to total protein.

Immunoprecipitation and pull-down. All the immunoprecipitation and pull-down experiments were conducted in *Drosophila* Kc167 cells adapted to serum-free culture medium (*Drosophila* Schneider Medium). Either full-length (Kr-h1 α-isoform) or partial gene products were cloned into *Drosophila* Gateway Vectors with N-terminal tags (FLAG and HA) following *Drosophila* Gateway Vectors protocols (https://emb.carnegiescience.edu/Drosophila-gateway-vector-collection). About 1 μg of constructs were transfected to 2×10^6 Kc167 cells using Effectene reagent (Qiagen, Hilden, Germany). Two days after transfection, cells were harvested and lysed in NP-40 lysis buffer (Thermo Fisher Scientific, Waltham, MA, USA) with proteinase inhibitors (Sigma-Aldrich, St Louis, MO, USA). To pull-down target proteins, total protein extracts were incubated with proper antibodies and Dynabeads Protein A (Thermo Fisher Scientific, Waltham, MA, USA). Following pull-down, western blotting was performed to examine protein complex. Antibodies used in pull-down and western blots include rabbit anti-Kr-h1 and anti-dFOXO produced in our laboratory, rabbit anti- HA (Covance, Dedham, MA, USA), and mouse anti-FLAG (Sigma-Aldrich, St Louis, MO, USA). Nuclear extracts for immunoprecipitation were conducted with a nuclear extraction kit (Active motif, Carlsbad, CA, USA).

Immunostaining and imaging. To examine the co-localization of Kr-h1 and dFOXO, larval fat body was dissected from fed or fasted 3rd instar larvae (90 hr AEL) (For fasting, larvae were placed onto wet kimwipe soaked with 1 × PBS for 16 hours). Tissue immunostaining were performed as previously described[47], using slow-Fade mounting solution with DAPI (Thermo Fisher Scientific, Waltham, MA, USA). Samples were imaged with a Zeiss 510 laser scanning confocal microscope or an Olympus BX51WI upright epifluorescence microscope equipped with Hamamatsu Flash 4.0 Plus CMOS Camera. Antibodies used in immunohistochemistry included: rabbit anti-Kr-h1 (1:200) (this study), anti-dFOXO (1:200)[75], anti-GFP (Sigma-Aldrich, St Louis, MO, USA), anti-rabbit IgG-DyLight 488 (1:300) anti-rabbit IgG-Alexa Fluor 594 (1:300) and anti-Guinea pig IgG-DyLight 488 (1:300) (Jackson ImmunoResearch, West Grove, PA, USA). Immunostaining of Kc167 cells was performed following above methods.

Chromatin immunoprecipitation (ChIP). ChIP was conducted as previously described[47]. About 50 staged larvae were used in each sample. Flies were homogenized and cross-linked in 1xPBS containing 1% formaldehyde. The fly nuclear extractions were sonicated using a Branson 450 sonicator to break down the chromatins. Immunoprecipitation was performed using Dynabeads Protein A and anti-Kr-h1 and anti-dFOXO antibodies. Following the wash with LiCl and TE buffer, the DNA-protein complex was eluted, reverse cross-linked, digested with Proteinase K and RNase. Kr-h1-bound or dFOXO-bound DNA fragments were purified and used as templates in qPCR analysis. Binding enrichment was calculated as the fold change between ChIP DNA vs. input DNA (Chromatin extracts before immunoprecipitation). The binding to the coding region of Actin (*Act5C*) was used as negative controls.

Juvenile hormone quantification. For each sample, 197–200 individual flies (7~10-day-old) were placed in 500 μl hexane in a glass vial with a Teflon cap insert and stored at −80 °C prior to analysis. To extract the hormone, the flies were crushed with a Teflon tissue grinder. The resultant homogenate was centrifuged at 3500 rpm for 5 min, and the supernatant was removed to clean vial. Extraction was conducted three times, combining the resultant supernatant from each sample. The gas chromatography/mass spectrometry (GC–MS) method[76], as modified[77,78], was used to quantify juvenile hormone (JH). Samples were eluted through aluminum oxide

columns successively with hexane, 10% ethyl ether–hexane and 30% ethyl ether–hexane. Samples were subjected to a second series of aluminum oxide elutions (30% ethyl ether-hexane then 50% ethyl-acetate–hexane) after derivatization with methyl-d alcohol (Sigma-Aldrich, St Louis, MO, USA) and trifluoroacetic acid (Sigma-Aldrich, St Louis, MO, USA). Purified samples were analyzed on an HP 7890A Series GC (Agilent Technologies, Santa Clara, CA, USA) equipped with a 30 m × 0.25 mm Zebron ZB-WAX column (Phenomenex, Torrence, CA, USA) and coupled to an HP 5975C inert mass selective detector with helium as the carrier gas. MS analysis occurred in the SIM mode, monitoring at m/z 76 and 225 to ensure specificity for the d3-methoxyhydrin derivative of JH III. Total abundance was quantified against a standard curve of derivatized JH III and using farnesol (Sigma-Aldrich, St Louis, MO, USA) as an internal standard. The detection limit is approximately 1 pg.

Statistical analysis. GraphPad Prism 6 (GraphPad Software, La Jolla, CA) was used for statistical analysis. To compare the mean value of treatment groups versus that of control, either student t-test or one-way ANOVA was performed using Dunnett's test for multiple comparison. The effects of mutants on starvation responses was analyzed by two-way ANOVA, including Tukey multiple comparisons test.

References

1. Tennessen, J. M. & Thummel, C. S. Coordinating growth and maturation - insights from *Drosophila*. *Curr Biol* **21**, R750–757 (2011).
2. Leopold, P. & Perrimon, N. *Drosophila* and the genetics of the internal milieu. *Nature* **450**, 186–188 (2007).
3. Wu, Q. & Brown, M. R. Signaling and function of insulin-like peptides in insects. *Annual review of entomology* **51**, 1–24 (2006).
4. Colombani, J., Andersen, D. S. & Leopold, P. Secreted peptide Dilp8 coordinates *Drosophila* tissue growth with developmental timing. *Science* **336**, 582–585 (2012).
5. Taniguchi, C. M., Emanuelli, B. & Kahn, C. R. Critical nodes in signalling pathways: insights into insulin action. *Nature reviews. Molecular cell biology* **7**, 85–96 (2006).
6. Calnan, D. R. & Brunet, A. The FoxO code. *Oncogene* **27**, 2276–2288 (2008).
7. Eijkelenboom, A. & Burgering, B. M. FOXOs: signalling integrators for homeostasis maintenance. *Nature reviews. Molecular cell biology* **14**, 83–97 (2013).
8. Colombani, J. *et al*. Antagonistic actions of ecdysone and insulins determine final size in *Drosophila*. *Science* **310**, 667–670 (2005).
9. Baumann, A. A. *et al*. Juvenile hormone and insulin suppress lipolysis between periods of lactation during tsetse fly pregnancy. *Mol Cell Endocrinol* **372**, 30–41 (2013).
10. Mirth, C. K. *et al*. Juvenile hormone regulates body size and perturbs insulin signaling in *Drosophila*. *Proc Natl Acad Sci USA* **111**, 7018–7023 (2014).
11. Hossain, M. S. *et al*. 20-Hydroxyecdysone-induced transcriptional activity of FoxO upregulates brummer and acid lipase-1 and promotes lipolysis in Bombyx fat body. *Insect biochemistry and molecular biology* **43**, 829–838 (2013).
12. Tatar, M. *et al*. A mutant *Drosophila* insulin receptor homolog that extends life-span and impairs neuroendocrine function. *Science* **292**, 107–110 (2001).
13. Sim, C. & Denlinger, D. L. Juvenile hormone III suppresses forkhead of transcription factor in the fat body and reduces fat accumulation in the diapausing mosquito, Culex pipiens. *Insect molecular biology* **22**, 1–11 (2013).
14. van der Vos, K. E. & Coffer, P. J. FOXO-binding partners: it takes two to tango. *Oncogene* **27**, 2289–2299 (2008).
15. Puigserver, P. *et al*. Insulin-regulated hepatic gluconeogenesis through FOXO1-PGC-1alpha interaction. *Nature* **423**, 550–555 (2003).
16. Seoane, J., Le, H. V., Shen, L., Anderson, S. A. & Massague, J. Integration of Smad and forkhead pathways in the control of neuroepithelial and glioblastoma cell proliferation. *Cell* **117**, 211–223 (2004).
17. Essers, M. A. *et al*. Functional interaction between beta-catenin and FOXO in oxidative stress signaling. *Science* **308**, 1181–1184 (2005).
18. Tiebe, M. *et al*. REPTOR and REPTOR-BP Regulate Organismal Metabolism and Transcription Downstream of TORC1. *Developmental cell* **33**, 272–284 (2015).
19. Koyama, T., Rodrigues, M.A., Athanasiadis, A., Shingleton, A.W. & Mirth, C.K. Nutritional control of body size through FoxO-Ultraspiracle mediated ecdysone biosynthesis. *eLife* **3** (2014).
20. Pecasse, F., Beck, Y., Ruiz, C. & Richards, G. Kruppel-homolog, a stage-specific modulator of the prepupal ecdysone response, is essential for *Drosophila* metamorphosis. *Developmental biology* **221**, 53–67 (2000).
21. Minakuchi, C., Zhou, X. & Riddiford, L. M. Kruppel homolog 1 (Kr-h1) mediates juvenile hormone action during metamorphosis of *Drosophila* melanogaster. *Mech Dev* **125**, 91–105 (2008).
22. Kayukawa, T. *et al*. Transcriptional regulation of juvenile hormone-mediated induction of Kruppel homolog 1, a repressor of insect metamorphosis. *Proc Natl Acad Sci USA* **109**, 11729–11734 (2012).
23. Kayukawa, T. *et al*. Kruppel Homolog 1 Inhibits Insect Metamorphosis via Direct Transcriptional Repression of Broad-Complex, a Pupal Specifier Gene. *J Biol Chem* **291**, 1751–1762 (2016).
24. Shi, L. *et al*. Roles of *Drosophila* Kruppel-homolog 1 in neuronal morphogenesis. *Developmental neurobiology* **67**, 1614–1626 (2007).
25. Fichelson, P., Brigui, A. & Pichaud, F. Orthodenticle and Kruppel homolog 1 regulate *Drosophila* photoreceptor maturation. *Proc Natl Acad Sci USA* **109**, 7893–7898 (2012).
26. Bieker, J. J. Kruppel-like factors: three fingers in many pies. *J Biol Chem* **276**, 34355–34358 (2001).
27. Kaczynski, J., Cook, T. & Urrutia, R. Sp1- and Kruppel-like transcription factors. *Genome biology* **4**, 206 (2003).
28. Turner, J. & Crossley, M. Cloning and characterization of mCtBP2, a co-repressor that associates with basic Kruppel-like factor and other mammalian transcriptional regulators. *The EMBO journal* **17**, 5129–5140 (1998).
29. van Vliet, J., Turner, J. & Crossley, M. Human Kruppel-like factor 8: a CACCC-box binding protein that associates with CtBP and represses transcription. *Nucleic Acids Res* **28**, 1955–1962 (2000).
30. Zhang, W., Kadam, S., Emerson, B. M. & Bieker, J. J. Site-specific acetylation by p300 or CREB binding protein regulates erythroid Kruppel-like factor transcriptional activity via its interaction with the SWI-SNF complex. *Molecular and cellular biology* **21**, 2413–2422 (2001).
31. Beck, Y., Pecasse, F. & Richards, G. Kruppel-homolog is essential for the coordination of regulatory gene hierarchies in early *Drosophila* development. *Developmental biology* **268**, 64–75 (2004).
32. Gronke, S. *et al*. Brummer lipase is an evolutionary conserved fat storage regulator in *Drosophila*. *Cell Metab* **1**, 323–330 (2005).
33. Bi, J. *et al*. Opposite and redundant roles of the two *Drosophila* perilipins in lipid mobilization. *Journal of cell science* **125**, 3568–3577 (2012).
34. Beller, M. *et al*. PERILIPIN-dependent control of lipid droplet structure and fat storage in *Drosophila*. *Cell Metab* **12**, 521–532 (2010).
35. Wang, B. *et al*. A hormone-dependent module regulating energy balance. *Cell* **145**, 596–606 (2011).
36. Puig, O., Marr, M. T., Ruhf, M. L. & Tjian, R. Control of cell number by *Drosophila* FOXO: downstream and feedback regulation of the insulin receptor pathway. *Genes & development* **17**, 2006–2020 (2003).

37. Yamamoto, R. & Tatar, M. Insulin receptor substrate chico acts with the transcription factor FOXO to extend *Drosophila* lifespan. *Aging Cell* **10**, 729–732 (2011).
38. Beck, Y., Dauer, C. & Richards, G. Dynamic localisation of KR-H during an ecdysone response in *Drosophila*. *Gene expression patterns: GEP* **5**, 403–409 (2005).
39. Hwangbo, D. S., Gershman, B., Tu, M. P., Palmer, M. & Tatar, M. *Drosophila* dFOXO controls lifespan and regulates insulin signalling in brain and fat body. *Nature* **429**, 562–566 (2004).
40. Minakuchi, C., Namiki, T. & Shinoda, T. Kruppel homolog 1, an early juvenile hormone-response gene downstream of Methoprene-tolerant, mediates its anti-metamorphic action in the red flour beetle Tribolium castaneum. *Developmental biology* **325**, 341–350 (2009).
41. Yamamoto, R., Bai, H., Dolezal, A. G., Amdam, G. & Tatar, M. Juvenile hormone regulation of *Drosophila* aging. *BMC biology* **11**, 85 (2013).
42. Hou, Y. *et al*. Temporal Coordination of Carbohydrate Metabolism during Mosquito Reproduction. *PLoS Genet* **11**, e1005309 (2015).
43. Xu, J., Sheng, Z. & Palli, S. R. Juvenile hormone and insulin regulate trehalose homeostasis in the red flour beetle, Tribolium castaneum. *PLoS Genet* **9**, e1003535 (2013).
44. Desvergne, B., Michalik, L. & Wahli, W. Transcriptional regulation of metabolism. *Physiol Rev* **86**, 465–514 (2006).
45. Webb, A. E. *et al*. FOXO3 shares common targets with ASCL1 genome-wide and inhibits ASCL1-dependent neurogenesis. *Cell Rep* **4**, 477–491 (2013).
46. Alic, N. *et al*. Genome-wide dFOXO targets and topology of the transcriptomic response to stress and insulin signalling. *Molecular systems biology* **7**, 502 (2011).
47. Bai, H., Kang, P., Hernandez, A. M. & Tatar, M. Activin signaling targeted by insulin/dFOXO regulates aging and muscle proteostasis in *Drosophila*. *PLoS Genet* **9**, e1003941 (2013).
48. van der Heide, L. P. & Smidt, M. P. Regulation of FoxO activity by CBP/p300-mediated acetylation. *Trends in biochemical sciences* **30**, 81–86 (2005).
49. Li, P. *et al*. AKT-independent protection of prostate cancer cells from apoptosis mediated through complex formation between the androgen receptor and FKHR. *Molecular and cellular biology* **23**, 104–118 (2003).
50. Dowell, P., Otto, T. C., Adi, S. & Lane, M. D. Convergence of peroxisome proliferator-activated receptor gamma and Foxo1 signaling pathways. *J Biol Chem* **278**, 45485–45491 (2003).
51. McConnell, B. B. & Yang, V. W. Mammalian Kruppel-like factors in health and diseases. *Physiol Rev* **90**, 1337–1381 (2010).
52. Rhee, D. Y. *et al*. Transcription factor networks in *Drosophila* melanogaster. *Cell Rep* **8**, 2031–2043 (2014).
53. Alland, L. *et al*. Identification of mammalian Sds3 as an integral component of the Sin3/histone deacetylase corepressor complex. *Molecular and cellular biology* **22**, 2743–2750 (2002).
54. Gray, S. *et al*. The Kruppel-like factor KLF15 regulates the insulin-sensitive glucose transporter GLUT4. *J Biol Chem* **277**, 34322–34328 (2002).
55. Gray, S. *et al*. Regulation of gluconeogenesis by Kruppel-like factor 15. *Cell Metab* **5**, 305–312 (2007).
56. Oishi, Y. *et al*. SUMOylation of Kruppel-like transcription factor 5 acts as a molecular switch in transcriptional programs of lipid metabolism involving PPAR-delta. *Nature medicine* **14**, 656–666 (2008).
57. Yusuf, I. *et al*. KLF4 is a FOXO target gene that suppresses B cell proliferation. *International immunology* **20**, 671–681 (2008).
58. Webb, A.E., Kundaje, A. & Brunet, A. Characterization of the direct targets of FOXO transcription factors throughout evolution. *Aging Cell* (2016).
59. Sheng, Z., Xu, J., Bai, H., Zhu, F. & Palli, S. R. Juvenile hormone regulates vitellogenin gene expression through insulin-like peptide signaling pathway in the red flour beetle, Tribolium castaneum. *J Biol Chem* **286**, 41924–41936 (2011).
60. Wang, X. *et al*. Hormone and receptor interplay in the regulation of mosquito lipid metabolism. *Proc Natl Acad Sci USA* **114**, E2709–E2718 (2017).
61. Jindra, M., Uhlirova, M., Charles, J. P., Smykal, V. & Hill, R. J. Genetic Evidence for Function of the bHLH-PAS Protein Gce/Met As a Juvenile Hormone Receptor. *PLoS Genet* **11**, e1005394 (2015).
62. Abdou, M. A. *et al*. *Drosophila* Met and Gce are partially redundant in transducing juvenile hormone action. *Insect biochemistry and molecular biology* **41**, 938–945 (2011).
63. Baumann, A. A. *et al*. Genetic tools to study juvenile hormone action in *Drosophila*. *Scientific reports* **7**, 2132 (2017).
64. Tatar, M., Bartke, A. & Antebi, A. The endocrine regulation of aging by insulin-like signals. *Science* **299**, 1346–1351 (2003).
65. Hsieh, P. N. *et al*. A conserved KLF-autophagy pathway modulates nematode lifespan and mammalian age-associated vascular dysfunction. *Nature communications* **8**, 914 (2017).
66. Rorth, P. A modular misexpression screen in *Drosophila* detecting tissue-specific phenotypes. *Proc Natl Acad Sci USA* **93**, 12418–12422 (1996).
67. Min, K. J., Yamamoto, R., Buch, S., Pankratz, M. & Tatar, M. *Drosophila* lifespan control by dietary restriction independent of insulin-like signaling. *Aging Cell* **7**, 199–206 (2008).
68. Ashok, M., Turner, C. & Wilson, T. G. Insect juvenile hormone resistance gene homology with the bHLH-PAS family of transcriptional regulators. *Proc Natl Acad Sci USA* **95**, 2761–2766 (1998).
69. Demontis, F. & Perrimon, N. FOXO/4E-BP signaling in *Drosophila* muscles regulates organism-wide proteostasis during aging. *Cell* **143**, 813–825 (2010).
70. Phillips, M. D. & Thomas, G. H. Brush border spectrin is required for early endosome recycling in *Drosophila*. *Journal of cell science* **119**, 1361–1370 (2006).
71. Rulifson, E. J., Kim, S. K. & Nusse, R. Ablation of insulin-producing neurons in flies: growth and diabetic phenotypes. *Science* **296**, 1118–1120 (2002).
72. Liu, Y. *et al*. Juvenile hormone counteracts the bHLH-PAS transcription factors MET and GCE to prevent caspase-dependent programmed cell death in *Drosophila*. *Development* **136**, 2015–2025 (2009).
73. Bai, H., Kang, P. & Tatar, M. *Drosophila* insulin-like peptide-6 (dilp6) expression from fat body extends lifespan and represses secretion of *Drosophila* insulin-like peptide-2 from the brain. *Aging Cell* **11**, 978–985 (2012).
74. Tennessen, J. M., Barry, W. E., Cox, J. & Thummel, C. S. Methods for studying metabolism in *Drosophila*. *Methods* **68**, 105–115 (2014).
75. Nechipurenko, I. V. & Broihier, H. T. FoxO limits microtubule stability and is itself negatively regulated by microtubule disruption. *J Cell Biol* **196**, 345–362 (2012).
76. Bergot, F. [Digestive utilization of purified cellulose in the rainbow trout (Salmo gairdneri) and the common carp (Cyprinus carpio)]. *Reproduction, nutrition, developpement* **21**, 83–93 (1981).
77. Srinivasan, A., Ramaswamy, S. B., Ihl Park, Y. & Shu, S. Hemolymph juvenile hormone titers in pupal and adult stages of southwestern corn borer [Diatraea grandiosella (pyralidae)] and relationship with egg development. *Journal of insect physiology* **43**, 719–726 (1997).
78. Brent, C. S. & Vargo, E. L. Changes in juvenile hormone biosynthetic rate and whole body content in maturing virgin queens of Solenopsis invicta. *Journal of insect physiology* **49**, 967–974 (2003).

Acknowledgements

We thank Bloomington *Drosophila* Stock Center, *Drosophila* Genomics Resource Center, and Vienna Drosophila Resource Center for fly stocks and cDNA clones. We thank Drs. Yannick Beck, Heather Broihier, Fabio Demontis, Tzumin Lee, Franck Pichaud, Geoff Richards, Eric Rulifson, Graham H. Thomas, Thomas Wilson for providing fly stocks and reagents. This work was supported by National Institutes of Health/National Institute on Aging grant R37 AG024360 to M.T., R00 AG048016 to H.B. Mention of trade names or commercial products in this publication is solely for the purpose of providing specific information and does not imply recommendation or endorsement by the U.S. Department of Agriculture. USDA is an equal opportunity provider and employer.

Author Contributions

Conceived and designed the experiments: M.T., H.B. Performed the experiments: P.K., K.C., Y.L., M.B., G.K., R.T., W.Z., S.P., C.S.B., H.B. Analyzed the data: P.K., K.C., C.S.B., M.T., H.B. Wrote the paper: C.S.B., S.L., M.T., H.B. All authors reviewed and approved the final version of this manuscript.

Additional Information

Supplementary information accompanies this paper at https://doi.org/10.1038/s41598-017-16638-1.

Competing Interests: The authors declare that they have no competing interests.

Publisher's note: Springer Nature remains neutral with regard to jurisdictional claims in published maps and institutional affiliations.